Spatiotemporal monitoring of a frequently-slip fault zone using downhole distributed acoustic sensing at the MiDAS Project

Huang, Hsin-Hua[1,2,*], Kou-Fong Ma[1,3,4], En-Shih Wu[5], Yun-Ze Cheng[1], Chin-Jen Lin[1], Chin-Shang Ku[1], Po-Li Su[1], and MiDAS working group

[1] Institute of Earth Sciences, Academia Sinica, Taipei, Taiwan
[2] Department of Geosciences, National Taiwan University, Taipei, Taiwan
[3] Department of Earth Sciences, National Central University, Taoyuan, Taiwan
[4] Earthquake-Disaster & Risk Evaluation and Management Center (E-DREaM), Taoyuan, Taiwan
[5] Institute of Oceanography, National Taiwan University, Taipei, Taiwan

Abstract

- The occurrence of seismic or aseismic slips on a fault is primarily controlled by fault zone structures and their properties. However, **the buried subsurface locations or strongly weathered outcrops of active faults** often pose a challenge for conducting high-resolution in-situ observations.
- The Milun fault ruptured both to the surface during the Hualien earthquakes of 1951 and 2018 in eastern Taiwan with a relatively well-known geometry, offering a unique venue to investigate the active fault zone using a cutting-edge **distributed acoustic sensing (DAS)** technique. DAS utilizes the interaction of photons with intrinsic defects of fiber to **translate the phase shift of scattering echoes into longitudinal dynamic strain** every few meters along the fiber, enabling continuous and high-resolution monitoring across the fault zone.
- The **Milun Fault Drilling and All-inclusive Sensing project (MiDAS),** launched in late 2021, drilled two holes in the **hanging wall (Hole A)** and **footwall (Hole B)** of the Milun fault and reached the fault zone at a depth of approximately 500 meters in Hole A. A 3-D fiber array including surface segments connecting two downhole fiber segments was deployed sequentially and completed in June 2022.

Introduction

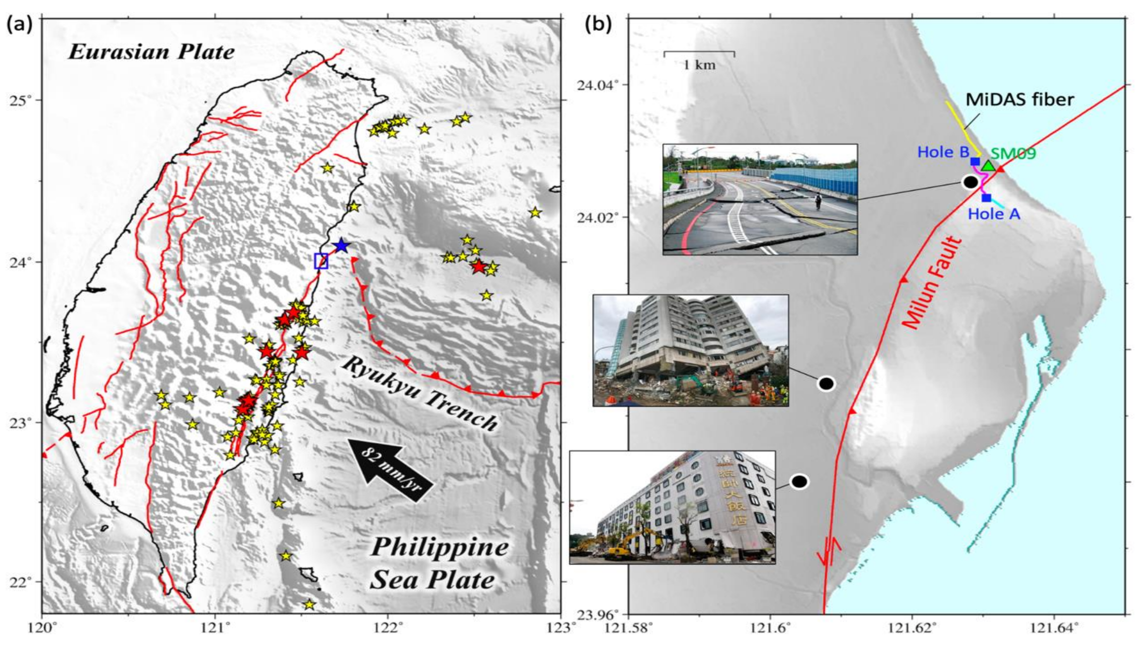

Figure 1 Taiwan regional tectonics and MiDAS project site. (a) Tectonic map showing Taiwan as a plate suture between the Eurasian Plate and the Philippine Sea Plate. Red lines indicate active faults. Blue box indicate the Hualien area stroke by the 2018 M_L6.4 Hualien earthquake (blue star). Yellow stars are collected earthquakes for analysis during the MiDAS operation time from January 2022 to January 2023, where red ones are used for Figure 5. (b) The Milun fault and damage photos caused by Hualien earthquake. The blue squares and colored lines are MiDAS drilling holes and fiber routes. Green triangle indicates a nearby geophone station SM09.

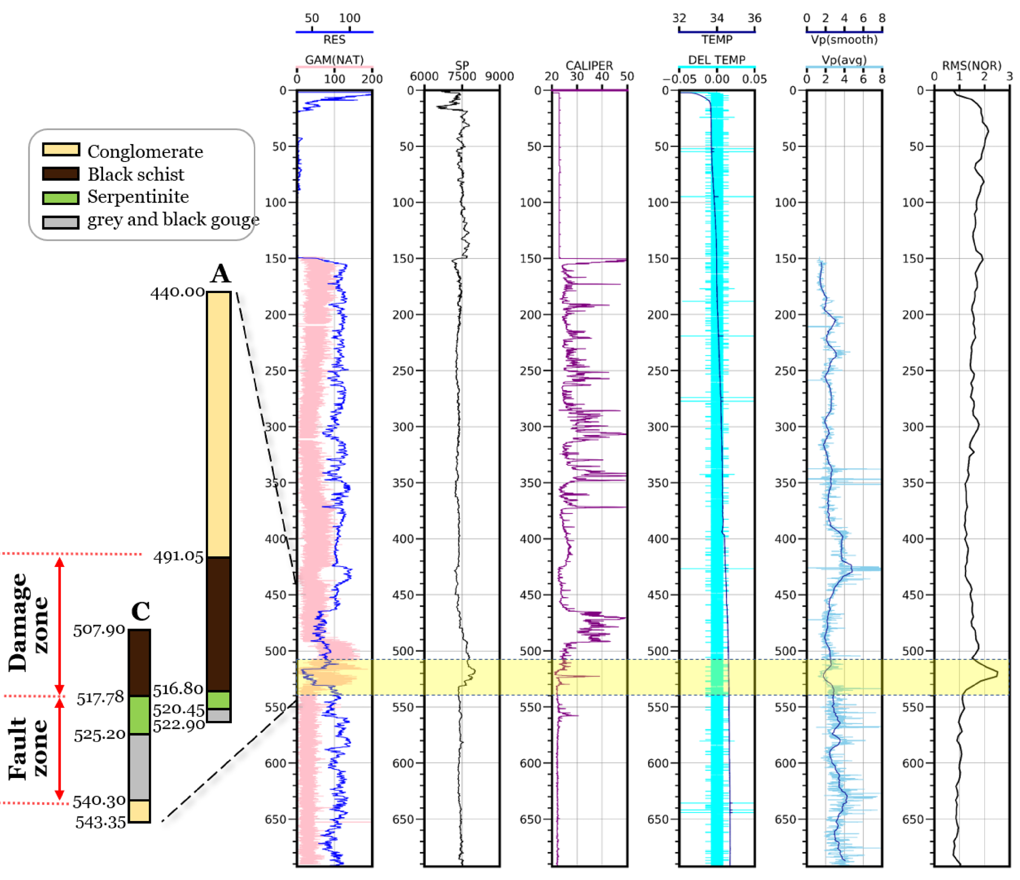

Figure 3 Seismic profile of DAS amplitude root-mean-square (RMS) ratios with coring and logging profiles for Hole A. Wireline logging at Hole A for (b) gamma ray and resistivity, (b) spontaneous potential, (c) caliper, (d) temperature, and (f) P-wave velocity. The measurements of 0-150 meters are influenced by the well casing. A lithological column based on coring at Hole A and close by Hole C (15 meters away from Hole A) at depths of 440-543 meters is indicated in (a). A DAS strain amplitude RMS ratio profile is derived in (g).

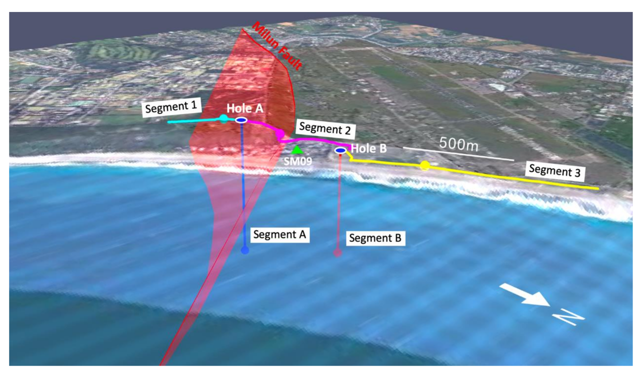

Figure 2 3-D perspective of MiDAS fiber array. Colored lines indicate different fiber segments deployed subsequently, with five dots as representative channel of each segment for analyses in Figure 6 and 8. Shaded red plane represents the schematic subsurface Milun fault plane. Green triangle indicates the geophone station SM09.

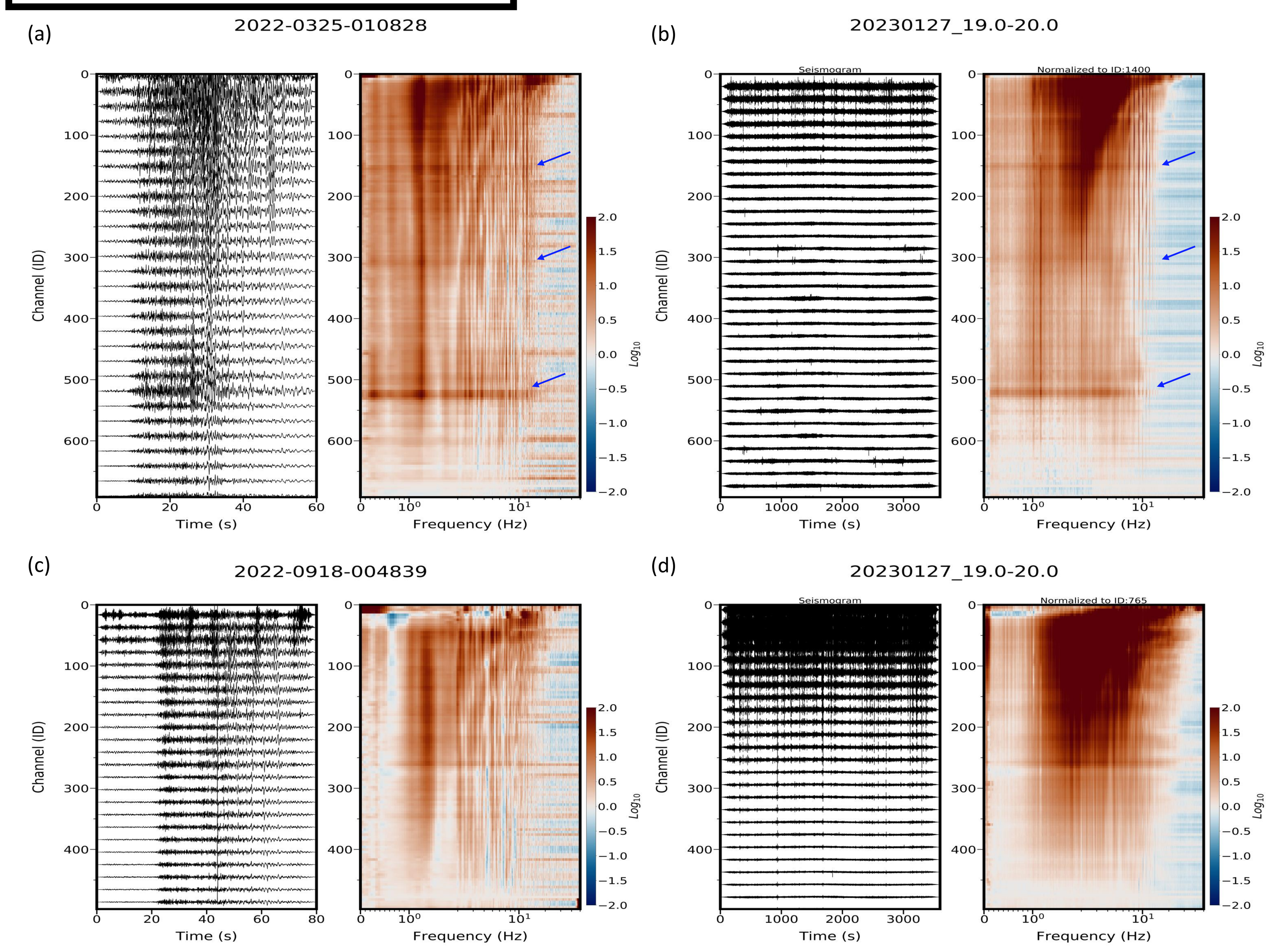

Figure 4 Depth-dependent spectral characteristics during strong motions (e.g. earthquakes) and weak motions at Hole A and Hole B. Left and right panels in (a-d) show the DAS strain rate waveforms and relative power spectral density (PSD) diagram. (a) and (b) are results of Hole A for an earthquake on 2022/03/25 with a 80-sec window and one hour ambient noise data on 2023/01/27 midnight Taiwan time. (c) and (d) are results of Hole B for an earthquake on 2022/09/18 with a 80-sec window and one hour ambient noise data on 2023/01/27 midnight Taiwan time.

Part1: Strong motion monitoring

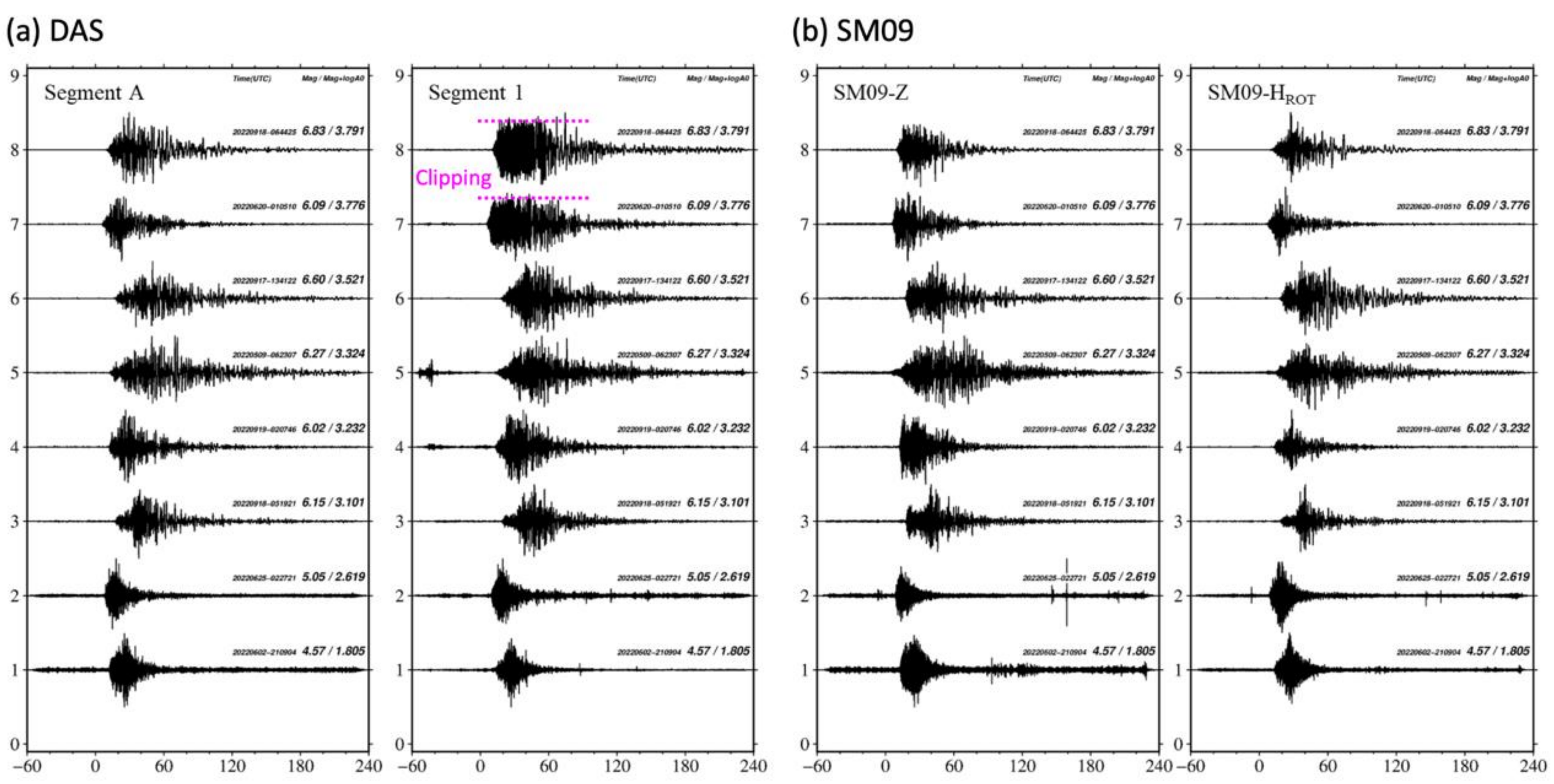

Figure 5 Waveform comparison for the selected earthquakes (red stars in Figure 1a) between the DAS strain rate data at representative channels of fiber segment A (vertical) and 1 (horizontal) and the acceleration data at the geophone SM09. The horizontal component of SM09 is rotated to the orientation of Segment 1. The pink dotted lines indicate the clipping phenomena observed in DAS data.

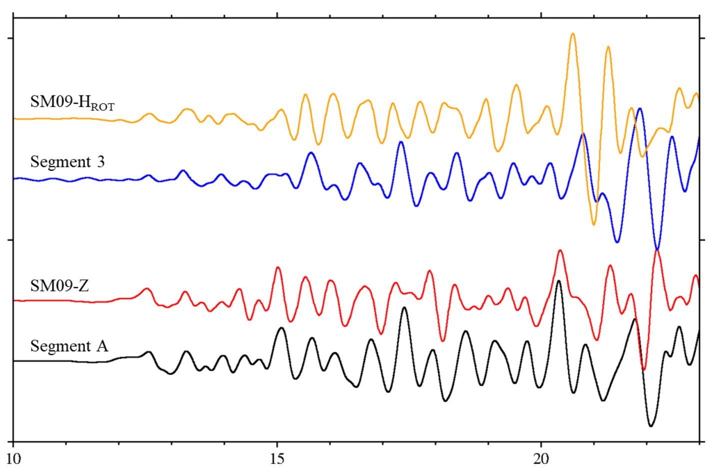

Figure 6 A Zoom-in waveform comparison between the DAS strain rate data and SM09 acceleration data for the 2022/09/19 earthquake. Both vertical and horizontal waveforms show a high similarity until the late coda.

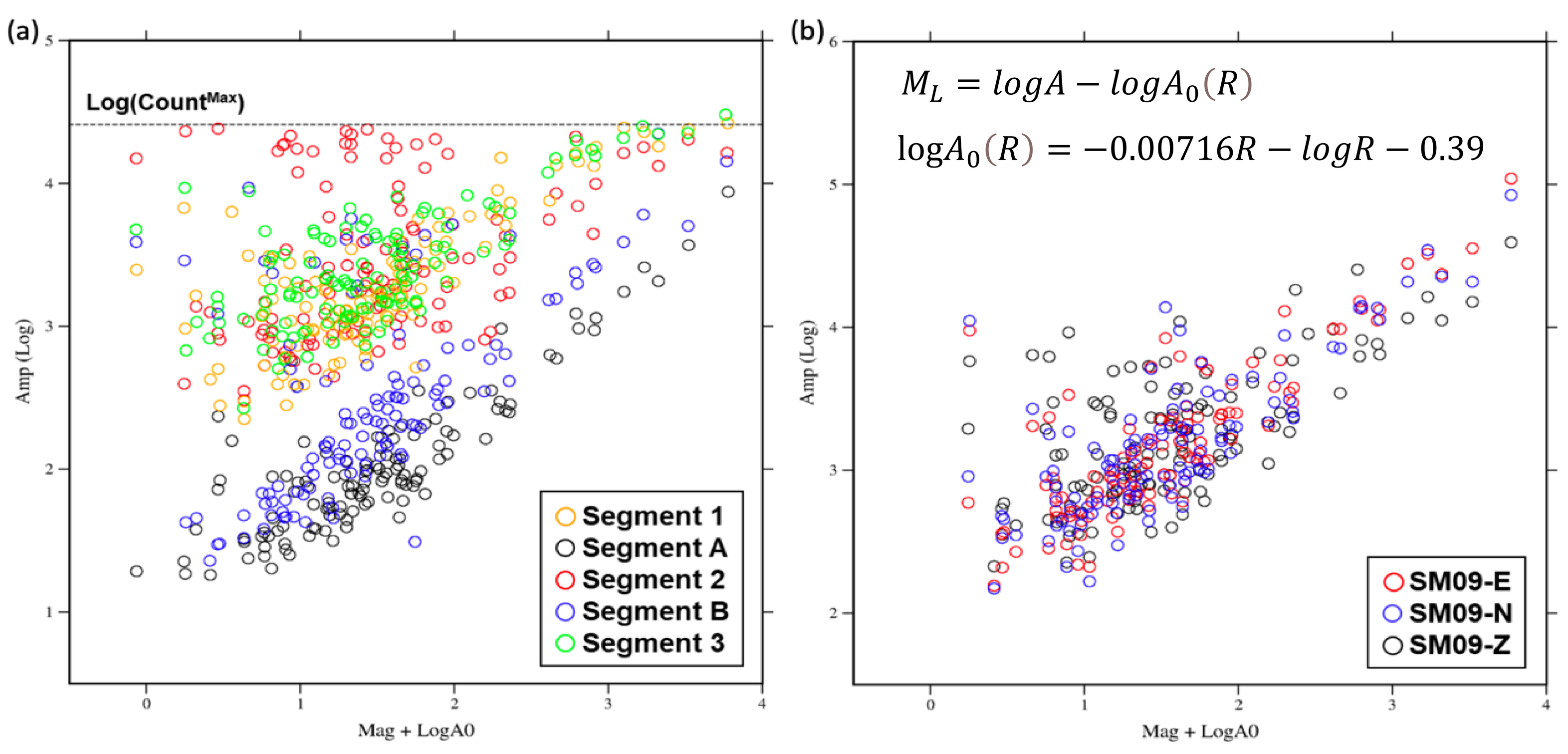

Figure 7 Peak ground motion attenuation relationship for the collected earthquakes (yellow stars in Figure 1a) between (a) the DAS strain rate data and (b) SM09 acceleration data. The analysis is conducted with the representative channels of five fiber segments as indicated by different colored circles in (a). The dotted black line denote the instrumental upper limit of strain rate. Results for the three components of SM09 are also shown in different colors in (b).

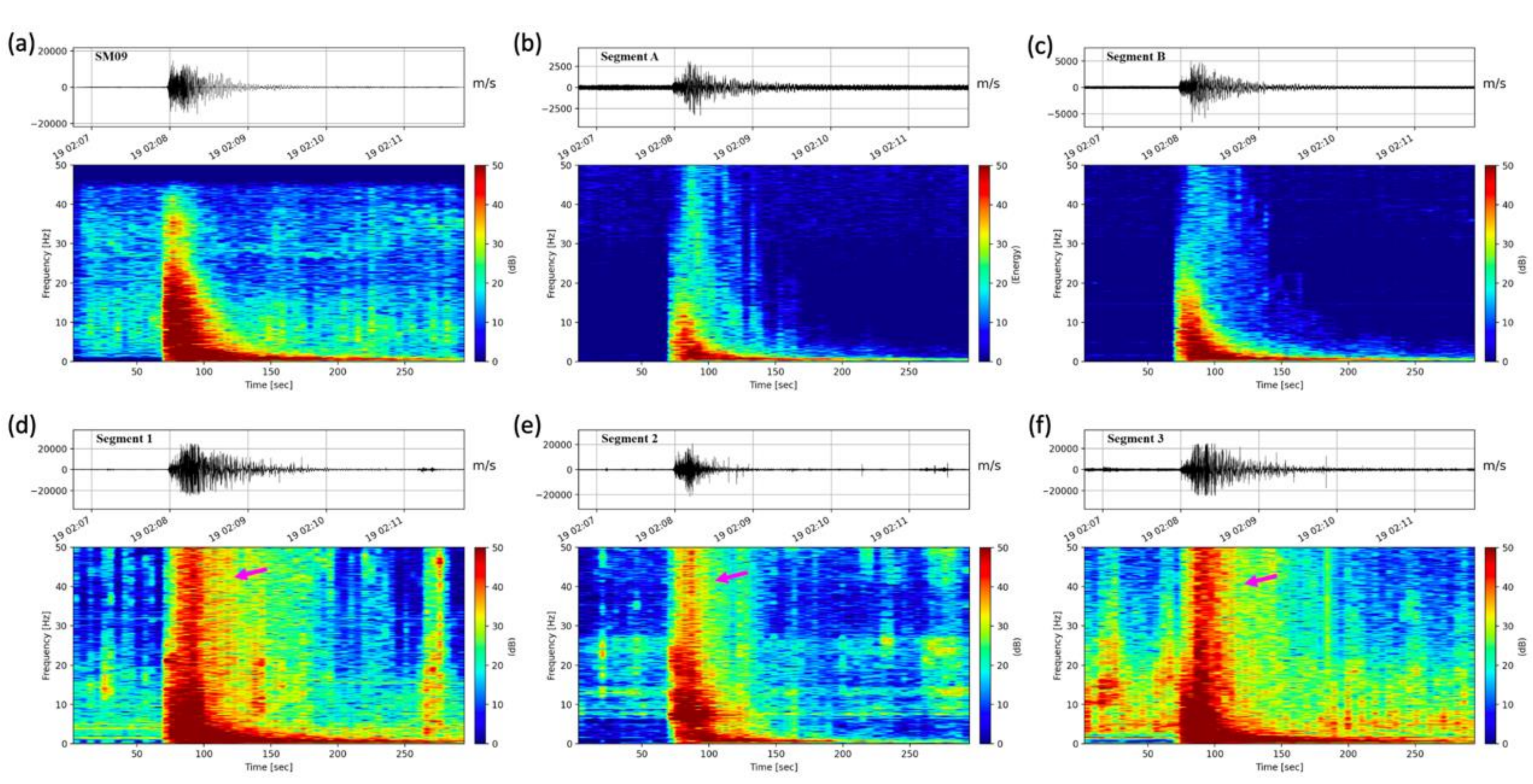

Figure 8 Spectrogram comparison for the 2022/09/19 earthquake between (a) the SM09 and (b-f) the representative channels of five fiber segments. The location of representative channels refers to Figure 2. (b-c) and (d-f) are downhole and surface segments, respectively. Pink arrows indicate the saturation effect at the horizontal fiber segments (d-f).

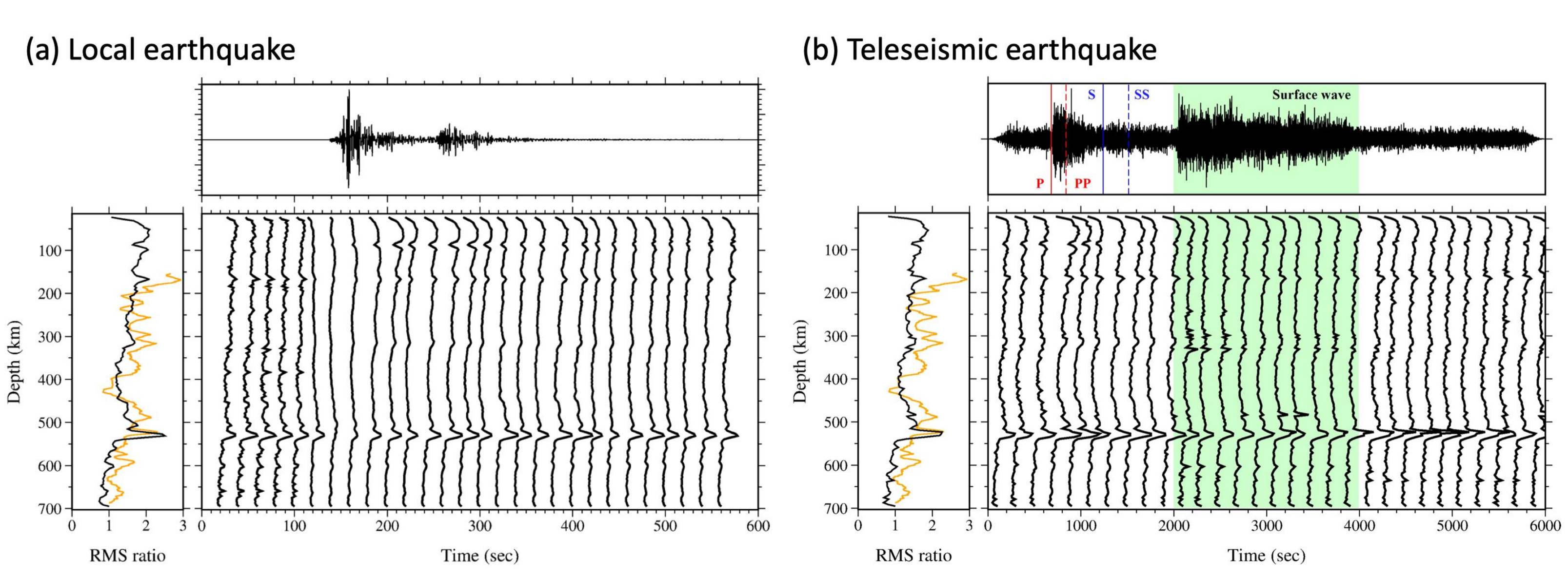

Figure 9 Temporal amplitude RMS ratio profiles at Hole A during (a) a M_L6.7 local earthquake on 2022/03/22 and (b) the M_W7.8 Turkey teleseismic earthquake on 2023/02/06. Upper panel shows the DAS strain-rate waveform, where the red and blue vertical lines and green shaded zones in (b) indicate the predicted P- and S-related arrivals and surface wave train. Lower panel shows the 20-s and 200-s moving-window calculation of amplitude RMS ratios for local and teleseismic events, respectively. Left panel shows the comparison between the mean amplitude RMS ratio profile (black) and logging P-wave slowness (1/velocity) profile (orange).

Part2: Weak motion monitoring

$$\dot{\varepsilon} = \frac{\ddot{u}}{c^a} = \frac{\cos\theta}{c}\ddot{u} = \frac{\cos\theta}{c} S * G(\theta) * A(\theta) \;\Rightarrow\; \frac{\dot{\varepsilon}_1}{\dot{\varepsilon}_2} = \frac{c_2 A_1(\theta)}{c_1 A_2(\theta)} = \frac{c_2'}{c_1'} \;\Rightarrow\; RMS(\dot{\varepsilon}) = \frac{1}{c} RMS(\ddot{u}\cos\theta)$$

$$\Rightarrow\; \frac{RMS(\dot{\varepsilon}_1)}{RMS(\dot{\varepsilon}_2)} = \frac{c_2'}{c_1'}$$

where $\dot{\varepsilon}$ is strain rate; $\ddot{u}$ is acceleration; and c^a and c are apparent and true phase velocity depending on the incident angle θ of seismic waves. Assuming $\ddot{u}$ is the convolution of source (S), path (G), and site-specific amplification terms (A) in Equation 1. Essentially, when the seismic wavefield $\ddot{u}$ can be recorded by the entire fiber array within a time window (regardless of phase shifts), the strain amplitude ratio between different channels will mainly reflect the ratio of elastic property (i.e. phase velocity in Equation 4) when local amplification effects are negligible.

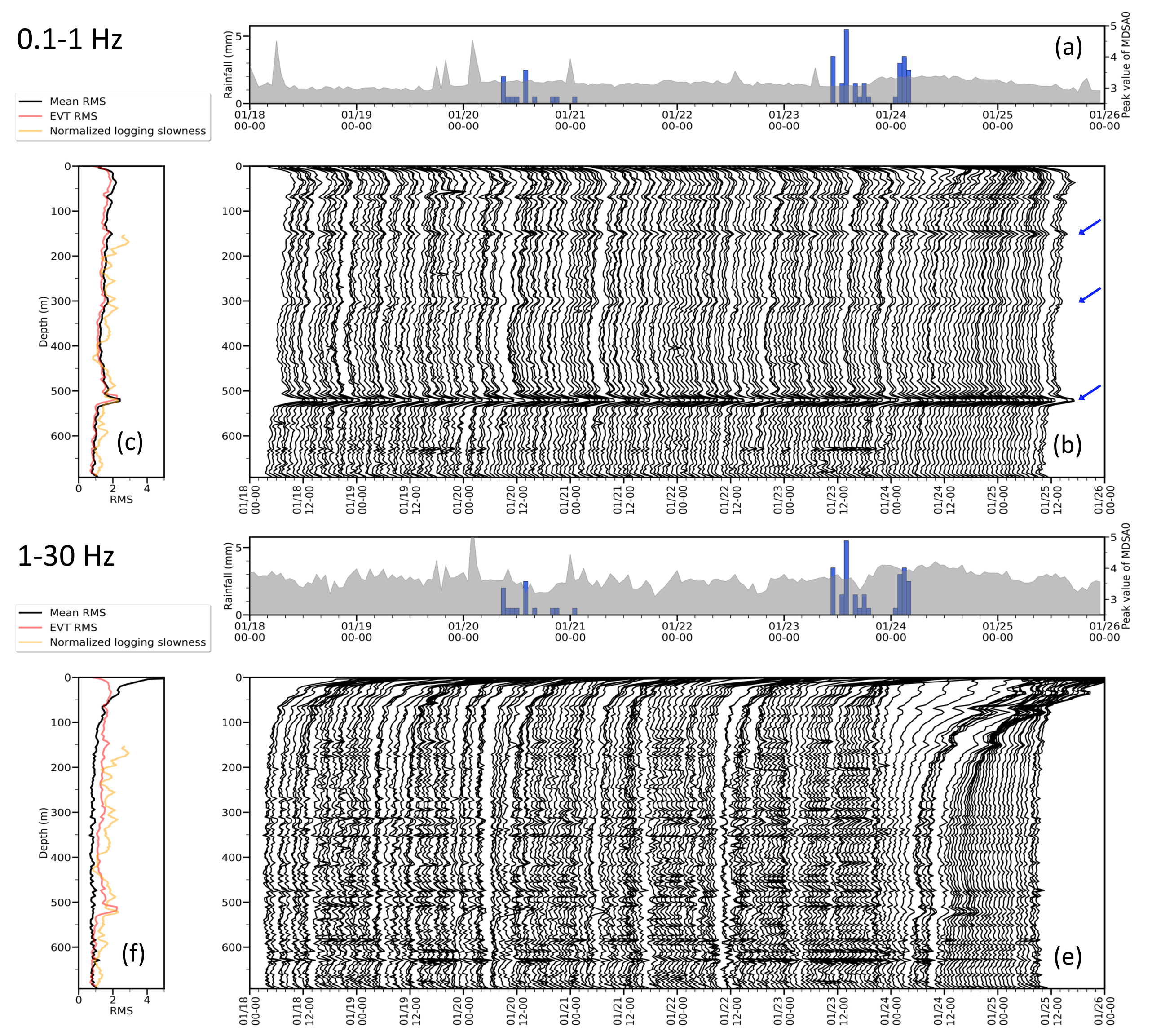

Figure 10 Long-term temporal amplitude RMS ratio profiles at Hole A from 18-25 January 2023 in (a-c) 0.1-1 Hz and (d-f) 1-30 Hz frequency bands. (a) and (d) show the hourly precipitation in blue bars and the hourly peak ground motions in gray. (b) and (e) show the hourly moving-window calculation of amplitude RMS ratios in corresponding frequency bands. (c) and (f) show the comparison between the mean amplitude RMS ratio profile (black), mean amplitude RMS ratio profile from earthquakes (red, Figure 11), and logging P-wave slowness (1/velocity) profile (orange).

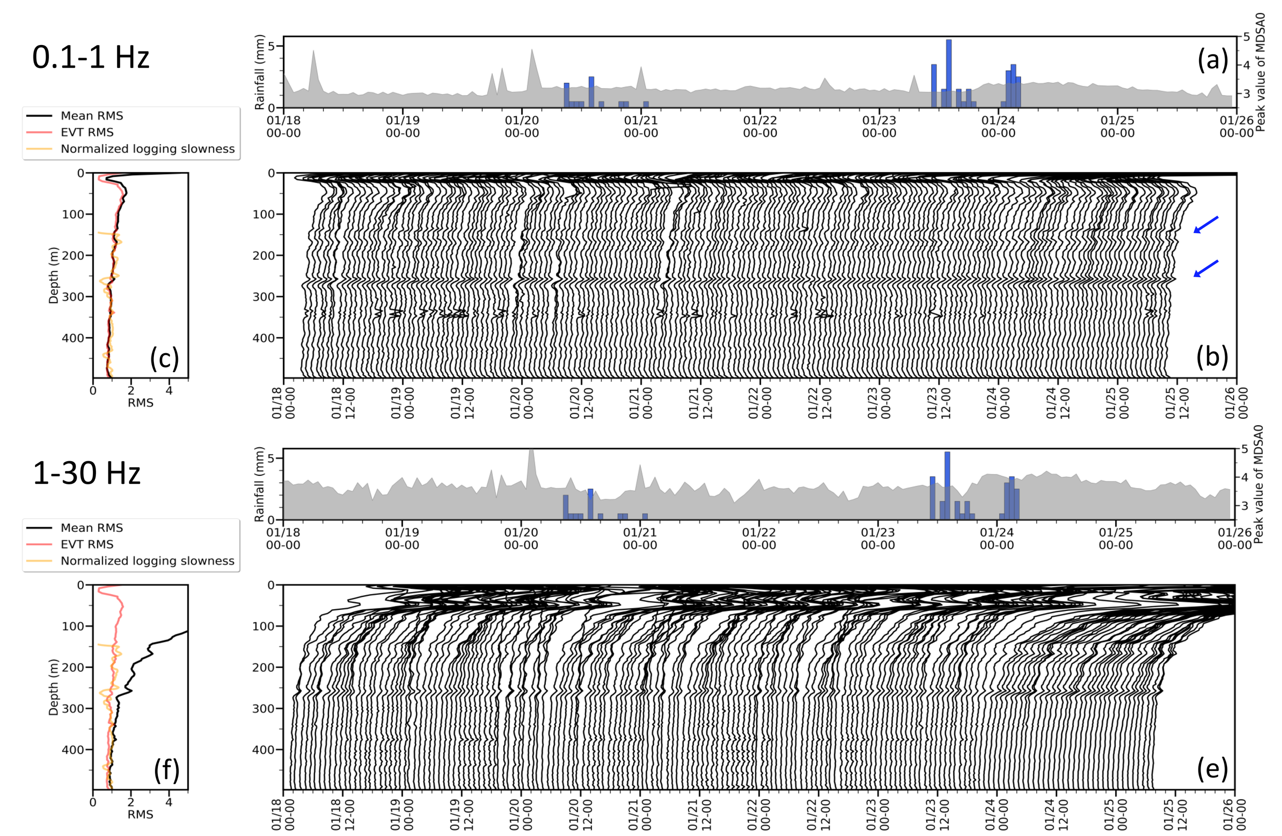

Figure 11 Long-term temporal amplitude RMS ratio profiles at Hole B from 18-25 January 2023 in (a-c) 0.1-1 Hz and (d-f) 1-30 Hz frequency bands. (a) and (d) show the hourly precipitation in blue bars and the hourly peak ground motions in gray. (b) and (e) show the hourly moving-window calculation of amplitude RMS ratios in corresponding frequency bands. (c) and (f) show the comparison between the mean amplitude RMS ratio profile (black), mean amplitude RMS ratio profile from earthquakes (red, Figure 11), and logging P-wave slowness (1/velocity) profile (orange).

Key points:

- **The MiDAS downhole fibers effectively monitor the frequently-slip Milun Fault with high spatiotemporal resolution.**
- **The DAS strain/strain rate data shares many similarities with seismograph velocity/acceleration data, informing the standard practices of earthquake monitoring and early warning.**
- **The RMS amplitude ratio method captures elastic property changes (e.g., slowness) with depth in long frequency bands (e.g. 0.1-1Hz), consistent with the logging P-wave velocity profile.**